JOURNAL OF MATERIAL SCIENCE 29 (1994) 5903–5910

Observations of the micro-mechanisms of fatigue-crack initiation in polycarbonate

T-J. CHEN, A. CHUDNOVSKY
Department of Civil Engineering, Mechanics and Metallurgy, University of Illinois at Chicago, P.O. Box 4348, Chicago, IL 60680, USA

C. P. BOSNYAK
The Dow Chemical Company, Polycarbonate and Blends Research, B-1470A, 2301 North Brazosport Boulevard, Freeport, TX 77541, USA

The mechanisms of crack initiation in tensile fatigue of single-edge notched specimens of polycarbonate of varying thickness have been elucidated. At low stresses and long times microcracking and localized yielding occurred to form regular diamond-shaped cells on a scale of 2–4 μm. On increasing the stress level with thin specimens (< 1 mm), the microshear bands coalesced to form macroscopic damage zones of yielded material around the notch, followed by crack tearing from the notch surface. With increasing specimen thickness, restriction of shear banding ensued and a stable, semi-elliptical cavitation, or pop-in, formed about 10–100 μm ahead of the notch, dependent on specimen geometry. As a result, the ligament formed between the notch and pop-in consists of yielded material. Brittle behaviour resulted with further increases in specimen thickness on loading, i.e. when the ligament could not be stabilized.

1. Introduction

In a previous paper the mechanisms of fatigue crack initiation were determined optically for single-edge notched specimens of polycarbonate in the thickness range 0.5–4.0 mm and used to assemble a map, Fig. 1 [1]. Three basic fatigue-crack initiation mechanisms were identified and named as cooperative ductile (at high stresses the damage zone formed ahead of a crack consisting of yielded material), solo-crack brittle (at large thicknesses very little damage-zone development), and cooperative brittle (identified as a cloud of micro-cracks which developed at the notch tip at low stresses in thin specimens). Two regions in the map were also characterized as having mixed initiation mechanisms. At intermediate thickness and low stresses, there was a mixed solo-crack with cooperative brittle failure, and at intermediate stresses and intermediate thicknesses cooperative ductile with solo-crack brittle failure. The time of fatigue-crack initiation is strongly dependent on micromechanisms of damage preceding the initiation. Under the same loading condition, the difference in the crack-initiation times up to four orders of magnitude is observed when the specimens varies between 0.2 and 4 mm thickness. Amongst the three basic failure-initiation mechanisms, the solo-crack brittle fracture mode is the least desirable for durable applications as it provides no warning of impending catastrophic fracture. In particular, polycarbonate is often selected for engineering applications, such as aircraft canopies, based on its reputation for impact toughness, and is expected to retain much of its toughness over the lifetime of the part. The understanding of the mechanisms of crack initiation is needed to develop appropriate failure criteria leading to proper design of polycarbonate in load-bearing applications. To achieve these, further observations at high magnification of the fractured specimens using optical and scanning electron microscopy (SEM), are reported and discussed in this paper.

We further discuss our observations of "pop-in", which is the sudden formation of a planar discontinuity ahead of a notch under certain loading conditions and thickness of polycarbonate. The pop-in phenomena has been reported in a notched specimen of polycarbonate under impact [2, 3], tension [4, 5] and bending tests [6–9] and is thought to consist of a planar disc of deformed material with approximate thickness 4–5 μm [3, 7]. The crack was reported subsequently to grow through this planar entity.

A difficulty with comparing our observations with studies of other workers is that they often did not report the important variables of polycarbonate molecular weight and processing or thermal history. In some cases, extruded sheet (presumably of higher molecular weight, weight average, $M_w \sim 35\,000$ $g\,mol^{-1}$) was employed of various thicknesses [5, 7], in others injection-moulded specimens [2, 9], but without stating the relationship of the notch direction to the frozen-in molecular orientation. Chang and Hsu [9] showed in their studies of slow bending of notched polycarbonate of molecular weights

0022–2461

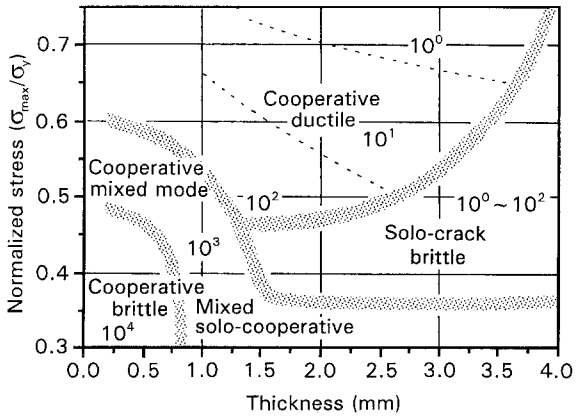

Figure 1 A fatigue initiation mechanism map for polycarbonate, M_w 29 000 g mol^{-1}.

$M_w \sim 20\,000$–$35\,000$ g mol^{-1}, and constant test conditions (notch tip radius 25 μm, thickness 3 mm, 25 °C), that a gradual change in mechanism from brittle to ductile occurred. At the lowest molecular weight the mechanism of failure was brittle with multiple cracked surfaces, whereas at the highest molecular weight a ductile zone formed and the crack formed by tearing through the yielded zone starting at the notch tip. With molecular weights in the range 24 000–30 000 g mol^{-1} the pop-in phenomena was observed. It is well known that increasing polycarbonate molecular weights, M_w, from 20 000 to 35 000 g mol^{-1} produces a slight lowering of its values of tensile modulus and yield stress, but the values of extension to break or fracture energy increase dramatically [9, 10].

The concept of the choice of initiation mechanism, broadly speaking ductile or brittle, being dependent on the competition between the yielding and cavitational response of the material to the loading history, has been well discussed in the literature [1–10]. Chau and Li [11, 12] have suggested that microcracks could form as a result of intersecting shear bands in many glassy polymers. Kitagawa [13] observed for a polycarbonate-extruded sheet (M_w unknown) that the critical notch-tip radius for ductile–brittle transition monotonically increased with increasing sheet thickness. Ma *et al.* [14] examined the modes of shear yielding in a notched polycarbonate of M_w 26 000 g mol^{-1} under slow tensile stress and with varying thickness. They reported that with increasing stress there is first a core yielding, which occurs at all thicknesses, then hinge shear and intersecting shear. A clear example of core shear yielding with intersecting shear bands looking from the notch face is given in their paper.

2. Experimental procedure

2.1. Material, specimen preparation and testing

The details of specimen preparation and testing in fatigue are given elsewhere [1]. Briefly, polycarbonate, M_w 29 000 g mol^{-1}, was provided by the Dow Chemical Company and specimens of thickness range 0.5–4.0 mm made using a Dake Compression Molder.

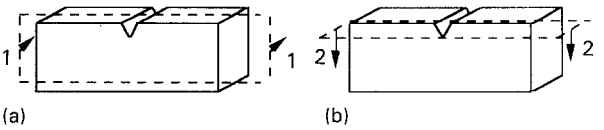

Figure 2 A sketch of the polishing direction: (a) side view, (b) top view.

Rectangular specimen 80 mm × 20 mm were cut from the sheets and 60° V-notch milled into the centre of one long edge with notch length 1 mm and notch radius 0.01 mm. Tension–tension fatigue experiments were conducted on a 1.1 ton capacity servohydraulic Instron testing system at room temperature. Sinusoidal waveform loading with frequency 1.0 Hz was used for fatigue testing. The tensile yield stress of PC, σ_y, was determined as 68 MPa using standard dog-bone geometry. The range of stress levels, SL, (σ_{max}/σ_y) were 0.35–0.75 and a stress ratio, R ($\sigma_{mim}/\sigma_{max}$) = 0.4.

The fractured specimens were sputter coated with gold/palladium and examined using a Jeol JSM-IC-845A scanning electron microscope (SEM) and 10 kV accelerating voltage. The observation was concentrated on the crack initiation area near the notch tip.

Two techniques were employed to study the pop-in phenomenon. In one case, three specimens of thickness 3.1 mm and with SL 0.45 were fatigued to first establish the crack initiation time, then four specimens were fatigued under the same conditions to the point just before crack initiation. In another case, specimens of thickness 3.1 mm under various stress levels 0.25–0.75 were tested under fatigue, but only for one cycle. The specimens were unloaded and polished using sand paper with grit sizes 200, 400 and 800 and alumina powder of size 0.1 and 0.05 μm in orthoganol directions as shown in Fig. 2. The specimens were observed optically using a Zeiss microscope to characterize the damage formation around the notch tip.

3. Observations

3.1. The micro-mechanisms of failure initiation

3.1.1. Cooperative brittle failure

Fig. 3a and b show micrographs of the fracture surface of the notch-tip region for a 0.7 mm thick specimen fatigued to complete failure under a constant normalized stress level, SL, of 0.35. The surface appears to resemble the fracture surface of a foamed structure. There is some indication in Fig. 3a of different regions which may have arisen from the crack initiating in different planes. However, similar features are seen within each region, as exemplified by Fig. 3b. The box in Fig. 3a indicates where the micrograph of higher magnification (Fig. 3b) originates. A regular array of cells is observed of approximately diamond shape. The acute angle of the diamond is around 75°. The overall cell size, as seen in Fig. 3b is around 2–4 μm with cell wall thicknesses around 0.2 μm. The cell walls are highly drawn with fibrillated tips.

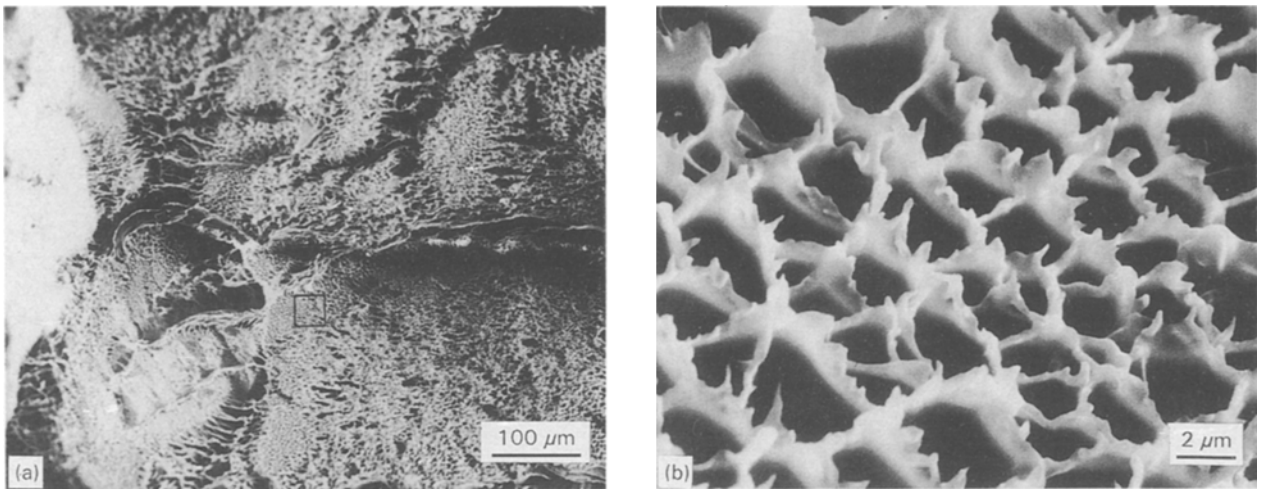

Figure 3 (a,b) SEM observations of the fracture surface of a cooperative brittle specimen in PC, $\sigma_{max}/\sigma_y = 0.35$, thickness 0.7 mm.

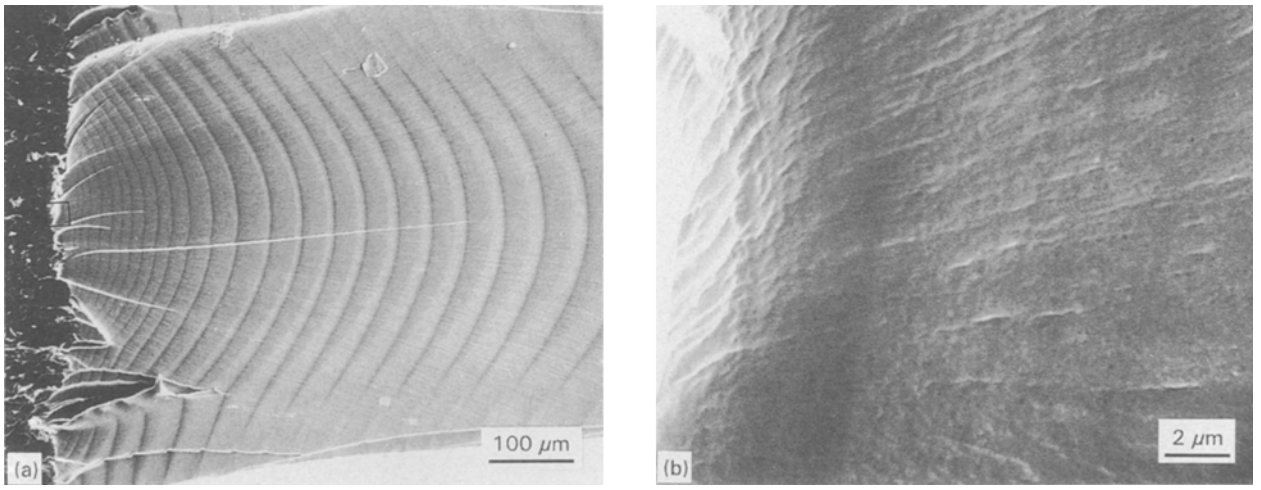

Figure 4 (a,b) SEM observations of the fracture surface of a cooperative ductile specimen in PC, $\sigma_{max}/\sigma_y = 0.75$, thickness 1.0 mm.

3.1.2. Cooperative ductile failure

Fig. 4a and b show the fracture surface of a specimen 1.0 mm thick fatigued to complete failure under SL 0.75, exhibiting the cooperative ductile failure initiation mechanism. In the crack propagation region below the notch plane, the polycarbonate has yielded and there is an overall reduction in surface width [1]. Looking at Fig. 4a, the crack appears to have initiated at several places along the deformed notch surface. Some triangular-shaped tears are evident which suggest that the crack also initiated in several planes. Striations, developed as a consequence of the crack advancement under fatigue, are clearly defined on the surface. In the crack-initiation region under higher magnification, Fig. 4b, the fracture surface is considered essentially featureless, although some traces of the crack path can be seen.

3.1.3. Solo-crack brittle failure

Fig. 5a and b are micrographs of the fracture surface of the notch-tip region for a 1.4 mm thick specimen fatigued to complete failure under SL 0.45. Similar features on the fracture surface of a notched polycarbonate have been described in previous studies [3, 5]. Four regions with different surface appearances can be observed. Starting from the original notch tip there appears to be a strip, or ridge region, traversing the thickness of the specimen and about 25 μm in width. The next region has a clearly defined initiation point, as illustrated in the higher magnification micrograph, Fig. 5b, where striations are seen on the fracture surface emanating from a crater. It is unclear if a material inhomogeneity, such as a dirt particle, coincident with the zone of high dilatational stress, caused this initiation site. The third region is a planar region, commonly known as a pop-in, whose fracture surface appears smoother than the initiation zone [2, 3, 6]. Finally, in region 4, as the crack is rapidly advancing in an unstable mode, a banded structure is seen, uniformly spaced every 10 μm, consisting of alternately coarse and fine pock-marked structure.

3.1.4. Mixed solo crack-cooperative ductile failure

Fig. 6a and b are micrographs of the fracture surface of the notch-tip region for a 1.0 mm thick specimen

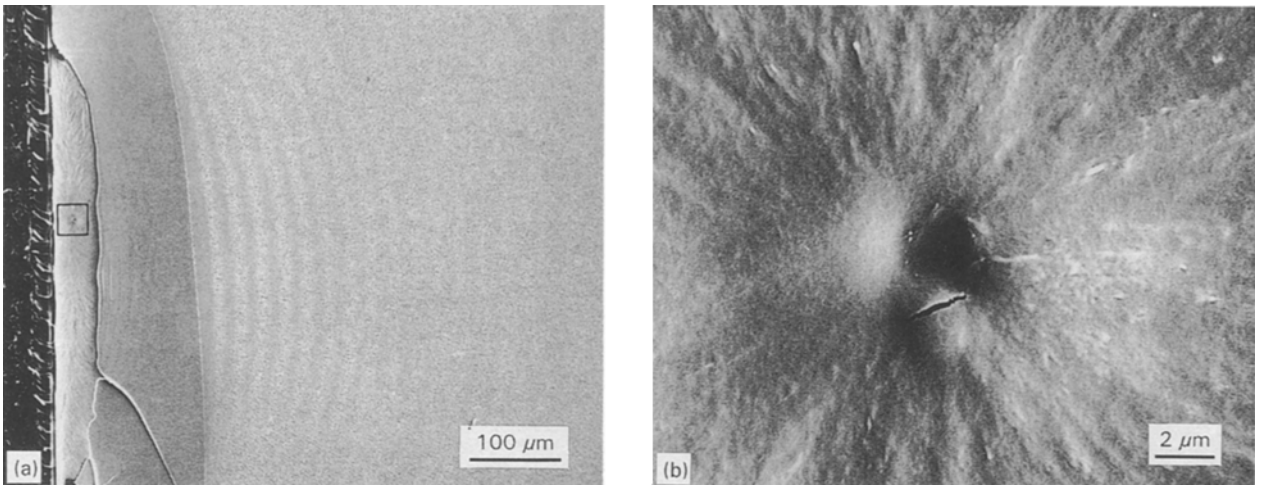

Figure 5 (a,b) SEM observations of the fracture surface of a solo-crack brittle specimen in PC, $\sigma_{max}/\sigma_y = 0.35$, thickness 1.4 mm.

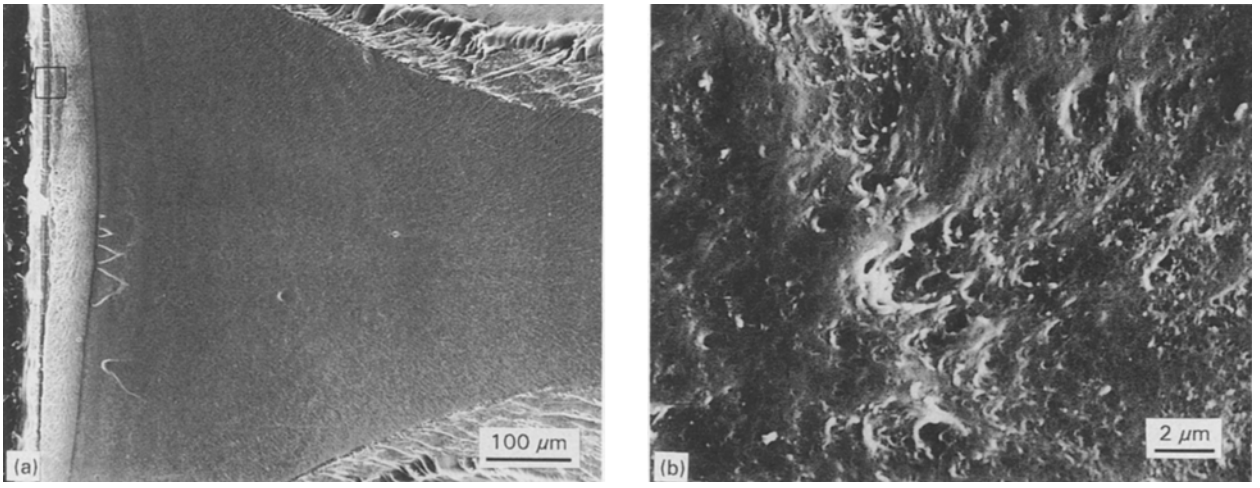

Figure 6 (a,b) SEM observations of the fracture surface of a mixed solo-crack and cooperative ductile specimen in PC, $\sigma_{max}/\sigma_y = 0.35$, thickness 1.0 mm.

fatigued to complete failure under SL 0.35. The fracture surface shows all the initiation characteristics previously described for solo-crack brittle failure, but as the planar crack of region 4 progressed, the sides of the specimen underwent ductile drawing and tearing. The crack-initiation region under higher magnification, Fig. 6b, shows it to be different from that of the solo-crack brittle type (Fig. 5b) by evidence of more microductility. The nature of the surface seen in Fig. 6b is suggestive of efforts of a failure mechanism similar to that seen in Fig. 3a.

Rotating the specimen 30°, one can see an interesting micrograph, Fig. 7a, with the original cut notch to the left. A ridge of material about 10 μm thick appears next to the cut notch. A smooth internal crack surface is located on a central plane and surrounded by ridges of drawn material. A side view of the same specimen, Fig. 7b, shows the irregular torn surfaces of the drawn material, the yielded zone of material below the plane of the notch, and microcracking on the side surface of the yielded zone. Higher magnification of the microcracking on the yielded zone side surface, Fig. 8a and b, suggests that planar sharp microcracks develop (~ 20 μm in length), perhaps along principal normal stress trajectories, then there is a microcrack–microcrack interaction producing a shear band between the microcrack tips. Of note, the polycarbonate is observed to undergo fibrillation in the microshear band with an inter-fibrillar distance of about 1–2 μm. There may be some similarity between this observed mechanism of fibrillation and that observed from the cooperative-brittle mechanism seen in Fig. 3b.

3.2. The damage zone in the solo-crack brittle fracture type specimens before catastrophic failure

Optical micrographs of a notched specimen of thickness 3.1 mm are shown in side view and rotated 30° before loading, Fig. 9a and b, and after application of one cycle to stress level $\sigma_{max}/\sigma_y = 0.45$, Fig. 9c and d, respectively. From the side-view optical micrograph, Fig. 9c, a small damage zone about 120 μm in length was apparent around the notch tip. On the 30° side-view picture, Fig 9d, a pop-in area is clearly visible near to the notch tip. Between this pop-in area and the notch tip is a narrow ligament of unbroken material.

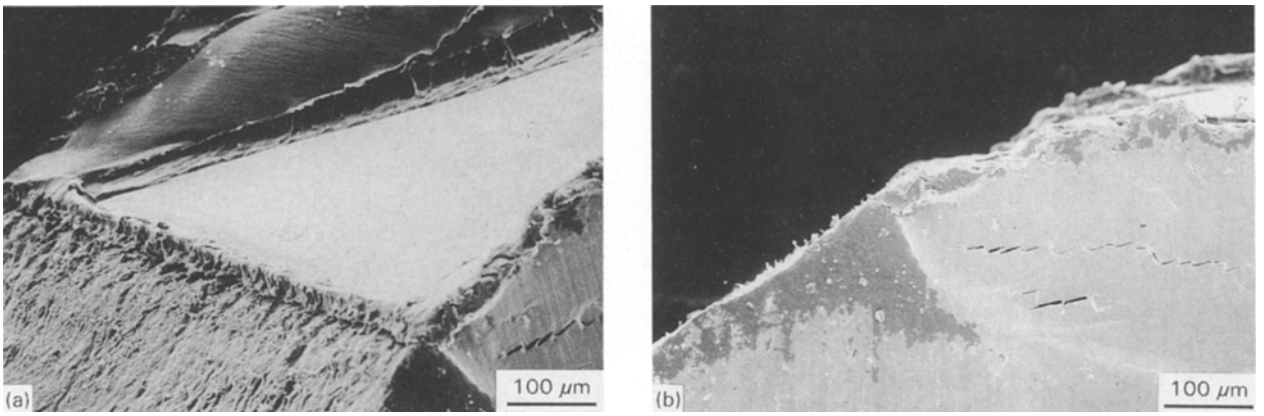

Figure 7 (a,b) SEM observations of the fracture surfaces of a mixed solo-crack and cooperative ductile specimen with 30° and 0° side views in PC, $\sigma_{max}/\sigma_y = 0.35$, thickness 1.0 mm.

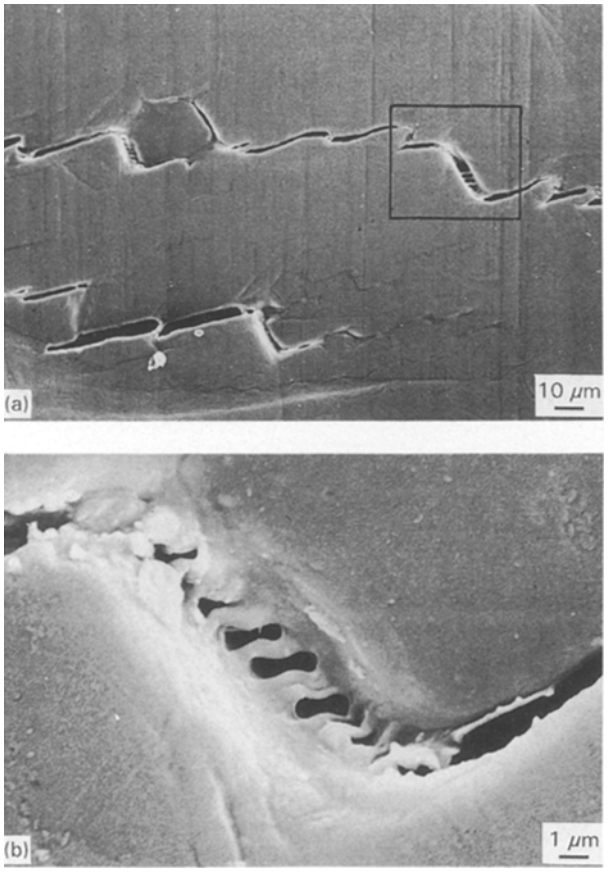

Figure 8 (a,b) SEM observations of the mixed solo-crack and co-operative ductile specimen side view in PC, $\sigma_{max}/\sigma_y = 0.35$, thickness 1.0 mm (under higher magnification).

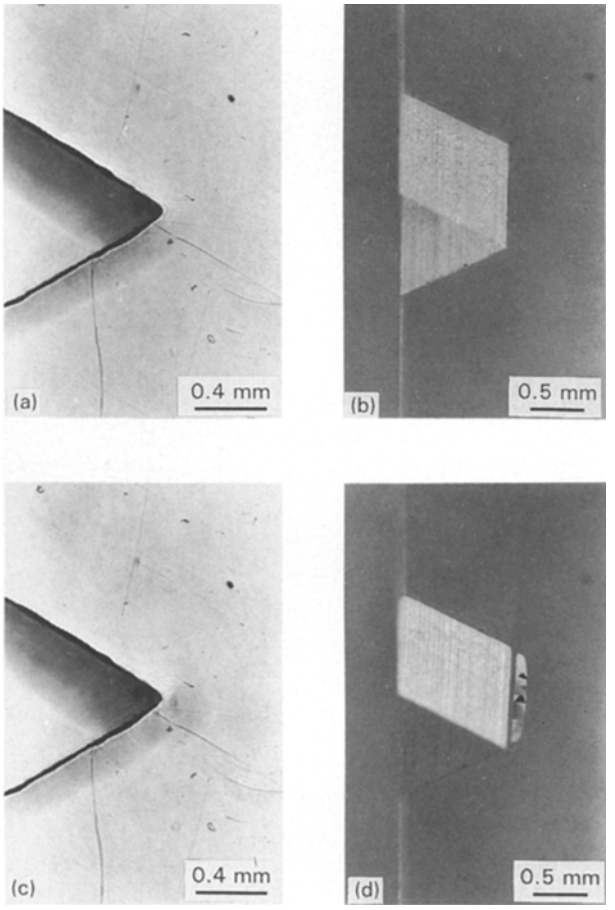

Figure 9 Specimen side view and 45° side view, (a, b) before testing, (c, d) after testing.

A clear illustration of the same phenomena was also presented by Mills [3].

Fig. 10 is a side-view optical micrograph of the pop-in region after unloading the specimen, polished in the plane of the width of the specimen (as shown in Fig. 2a). It shows that the pop-in area is composed of several, approximately parallel, regularly spaced crazes or micro-cracks ahead of the notch tip. Fig. 11a and magnifications in Fig. 11b–d are views of the pop-in area as seen through the notch tip. They support the observation in Fig. 10 that the crazes or micro-cracks are not in the same plane and also that no one craze, or microcrack, traverses the whole thickness of the specimen. The craze tips or micro-crack tips initially overlap, then join, according to Fig. 11c and d. Ishikawa *et al.* [7], in their studies of a 6 mm thick polycarbonate sheet (of an undisclosed molecular weight and thermal history), showed that many semi-elliptical entities with different sizes and thickness were formed ahead of a notch tip, and recognized that they were in different planes [8].

3.3. The pop-in phenomena in the single-cycle fatigue test with varied stress level

Fig. 12 shows the dynamic sequence of crack initiation with increasing load level. More specifically, these are side-view optical pictures of surface-polished 3.1 mm thick specimens under single-cycle fatigue test with SL 0.25–0.75. For the specimen under SL 0.25 (Fig. 12f) a damage zone of dimensions less than 15 μm was recorded at the notch tip, but no pop-in phenomena.

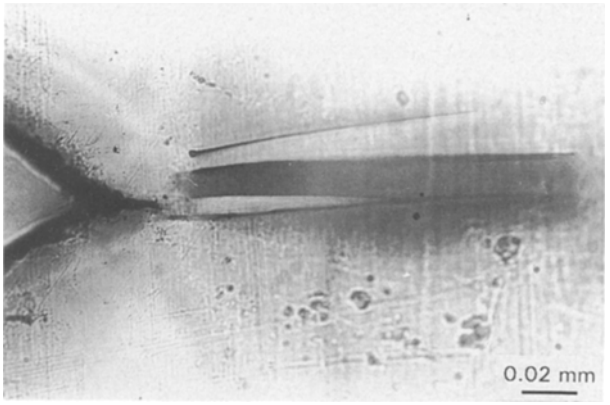

Figure 10 The side-view appearance of pop-in phenomena in the polished specimen, prior to catastrophic failure.

Above SL 0.35, the pop-in occurred with length ~ 50 μm and the unbroken ligament can be clearly identified. At SL 0.45 the presence of a second pop-in entity is observed on a different plane from the first, but of similar length, ~ 100 μm. The ligament size, from the initial notch surface to the beginning of the pop-in, once formed does not change significantly with increasing stress levels. The crack initiated from the notch root at SL 0.55. i.e. by fracture of the ligament, but from a position slightly deviated from the notch tip. Coincident with the crack formation is the presence of shear bands on the surface. Interestingly, at SL 0.65 and 0.75, the crack does not appear to grow through the pop-in areas formed at lower stresses and, in fact, the initially formed pop-in areas continue to grow with increasing stress level while the crack is growing.

4. Discussion

The observation of the formation of an array of diamond-shaped cells on the surface of the polycarbonate formed at low fatigue stresses and long fatigue-cycle times (greater than 10^4 cycles before crack initiation), seen in Fig. 3b, appears to be novel, although remnants of craze structure have been reported [2, 3]. The microshear bands of extruded sheet polycarbonate ahead of a notch were observed to be

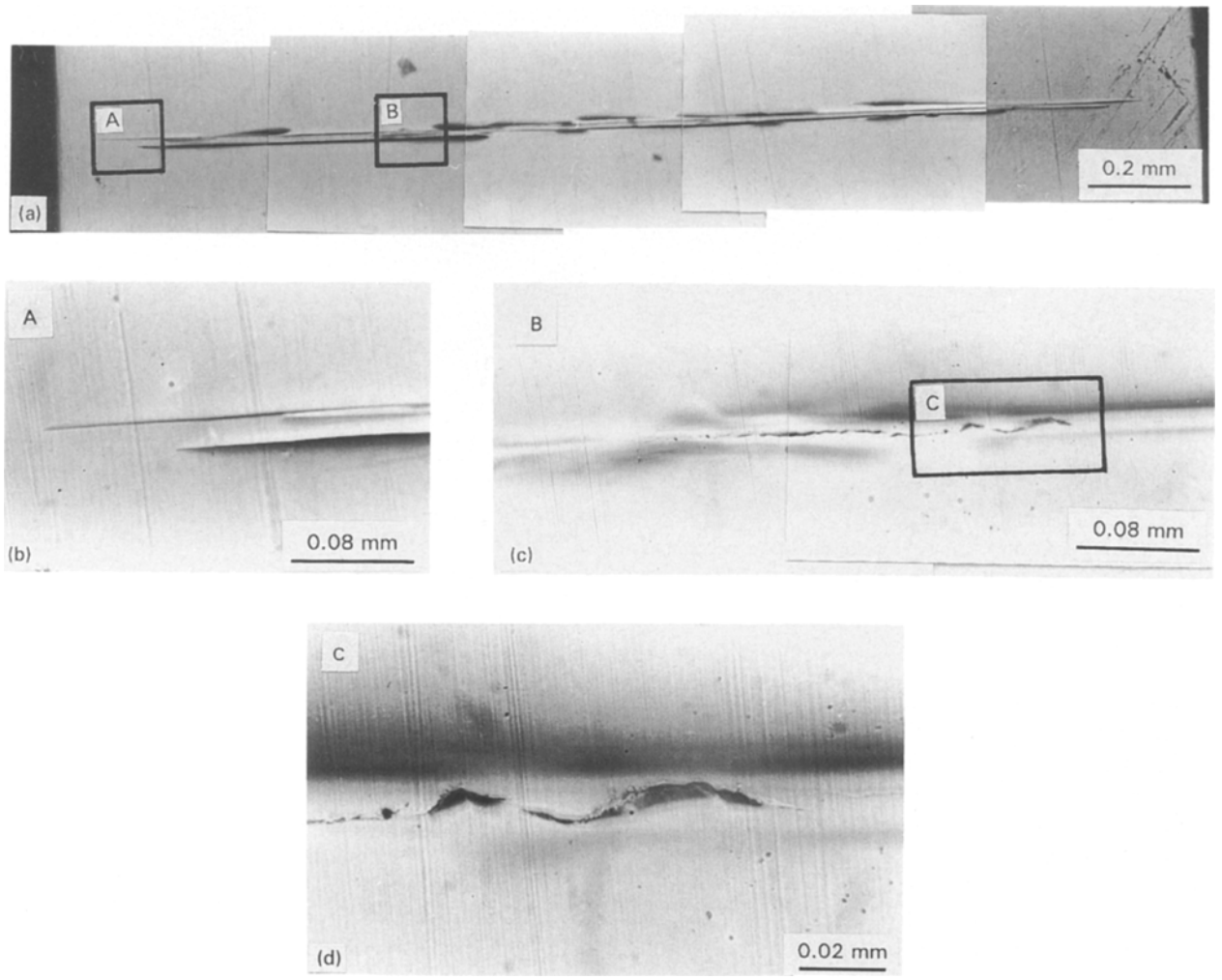

Figure 11 The top-view appearance of pop-in phenomena in the polished specimen, prior to catastrophic failure.

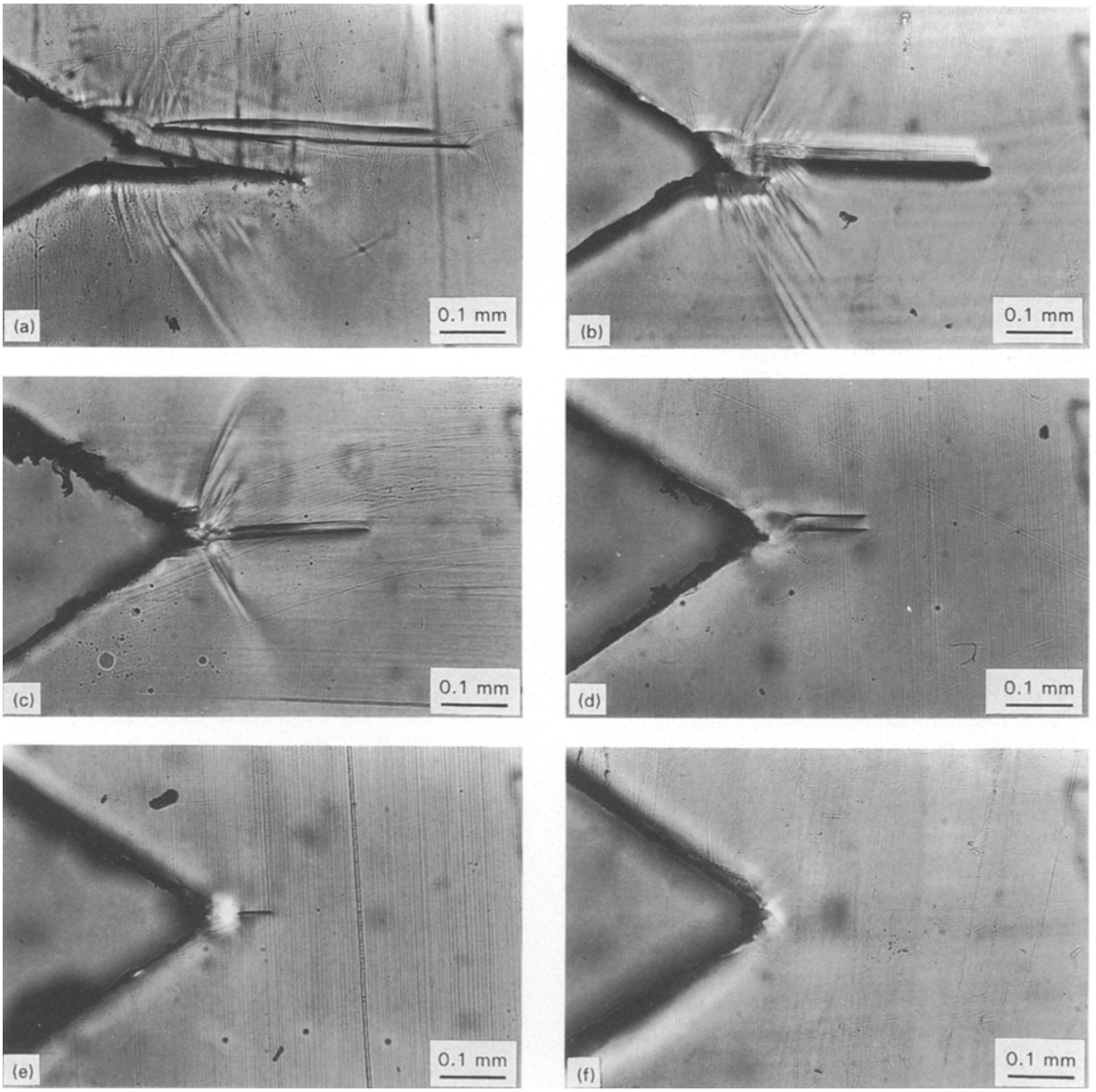

Figure 12 The side-view appearances of the pop-in region in the polished specimen for varied stress level, after the first fatigue loading cycle. (a) SL 0.75 (b) SL 0.65, (c) SL 0.55, (d) SL 0.45, (e) SL 0.35, (f) SL 0.25.

approximately 3–5 μm apart [6, 13] and if, as Chau and Li have suggested, that microcracks form as a result of intersecting shear bands [11, 12], then the combination of these two mechanisms could explain our observation for the array and scale of structure. However, formation of shear banding is usually symmetrical around the mid-plane of a notch and so the above explanation would not account fully for the asymmetry of the damage zone microcracks or crazes associated with the main crack development, reported previously [1].

At high loading, the thinner notched specimens preferred to yield at the notch tip, forming large deformation zones spanning the entire thickness, followed by tearing from the deformed notch surface. In our terminology this mechanism is called cooperative ductile failure and the sequence of damage formation appears to be similar to that well described by Ma *et al.* [14].

With increasing specimen thickness, a plane strain constraint is imposed at the core of the specimen. This leads to the pop-in phenomena. Application of Hill's slip-line theory [15] appears to be useful in determining the position of the nucleus of the pop-in [7, 13]. A ligament of deformed material is thus formed simultaneously with the pop-in [4]. The pop-in relieves some of the constraint, thereby allowing shear yielding to occur in the remaining material. The subsequent growth of the pop-in region in the early stages is therefore controlled not only by the resistance to new surface generation, but also by elements governing deformation and breakage of the ligament, for example, the chance initiation of fracture by a defect such as a dirt particle, present in all materials. With increasingly thicker specimens, brittle behaviour via solo-crack formation became prevalent as the ability to relieve the stresses by shear deformation is increasingly restricted. A necessary feature for ductility in

polycarbonate appears to be the initial formation of elementary shear bands on the 2–4 μm scale. A knowledge of how these elementary shear bands develop from the underlying molecular structure would be highly desirable, but remains elusive at present.

5. Conclusion

The initiation regions of fracture surfaces of polycarbonate fatigued under various thickness and stress level have been carefully analysed by optical and scanning electron microscopy. At low stresses and long times the fracture surface showed evidence of microcracking and localized yielding to form regular diamond-shaped cells on a scale of 2–4 μm. On increasing the stress level with thin specimens (< 1 mm), the microshear bands coalesced to form macroscopic damage zones around the notch followed by crack tearing from the notch surface.

With increasing specimen thickness, restriction of shear banding ensued and a stable cavitation, or pop-in, formed ahead of the notch together with formation of a ligament of yielded material between the notch surface and the pop-in. The pop-in was observed to consist of several thin, semi-elliptical crazes or microcracks in different planes, whose tips initially overlap. Solo-crack brittle behaviour ensued with further increases in specimen thickness, i.e. when the ligament could not be stabilized. Thus, for appropriate normalization factors for the newly developed fatigue-initiation mechanism map for polycarbonate, the kinetics of shear-band formation under controlled loading conditions need to be determined.

Acknowledgements

The authors thank Dr C-I. Kao, the Dow Chemical Co., for the helpful discussions, E. Garcia-Meitin, The Dow Chemical Co., and Z. Zhou, University of Illinois at Chicago, for their photomicrograph support, and the Dow Chemical Co. for financial support of this work.

References

1. T-J. CHEN, C. P. BOSNYAK and A. CHUDNOVSKY, *J. Appl. Polym. Sci.*, **49** (1993) 1909.
2. D. HULL and T. W. OWEN, *J. Polym, Sci. Polym. Phys. Ed.* **1** (1973) 2039.
3. N. J. MILLS, *J. Mater. Sci.* **11** (1976) 363.
4. A. KIM, C. P. BOSNYAK and A. CHUDNOVSKY, *J. Appl. Polym. Sci.*, **49** (1993) 885.
5. H. NISITANI and H. HYAKUTAKE, *Eng. Fract. Mech.* **22** (1985) 359.
6. D. G. LéGRAND, *J. Appl. Polym. Sci.* **13** (1969) 2129.
7. M. ISHIKAWA, I. NARISAWA and H. OGAWA. *J. Polym. Sci. Polym. Phys. Ed.* **15** (1977) 1791.
8. M. ISHIKAWA and I. NARISAWA, *J. Mater. Sci.* **18** (1983) 2826.
9. F-C. CHANG and H-C. HSU, *J. Appl. Polym. Sci.* **43** (1991) 1025.
10. M. PARVIN and J. G. WILLIAMS, *Int. J. Fract.* **11** (1975) 963.
11. C. C. CHAU and J. C. M. LI, *J. Mater. Sci.* **14** (1979) 1593.
12. *Idem, Ibid.* **14** (1979) 2172.
13. M. KITAGAWA, *Ibid.* **17** (1982) 2514.
14. M. MA, K. VIJAYAN, A. HILTNER and E. BAER, *Ibid.* **24** (1989) 2687.
15. R. HILL, *Q. J. Mech. Appl. Maths.* **2** (1949) 40.

Received 11 August 1993
and accepted 5 May 1994